NANO LETTERS

pubs.acs.org/NanoLett

Letter

# On-Demand Opioid Effect Reversal with an Injectable Light-Triggered Polymer-Naloxone Conjugate

Wei Zhang, Dali Wang, Claire A. Ostertag-Hill, Yiyuan Han, Xiyu Li, Yueqin Zheng, Berwyn Lu, and Daniel S. Kohane*

Cite This: *Nano Lett.* 2023, 23, 10545−10553

Read Online

ACCESS | Metrics & More | Article Recommendations | Supporting Information

**ABSTRACT:** Misuse of opioids can lead to a potential lethal overdose. Timely administration of naloxone is critical for survival. Here, we designed a polymer−naloxone conjugate that can provide on-demand phototriggered opioid reversal. Naloxone was attached to the polymer poly(lactic-*co*-glycolic acid) via a photocleavable coumarin linkage and formulated as injectable nanoparticles. In the absence of irradiation, the formulation did not release naloxone. Upon irradiation with blue (400 nm) light, the nanoparticles released free naloxone, reversing the effect of morphine in mice. Such triggered events could be performed days and weeks after the initial administration of the nanoparticles and could be performed repeatedly.

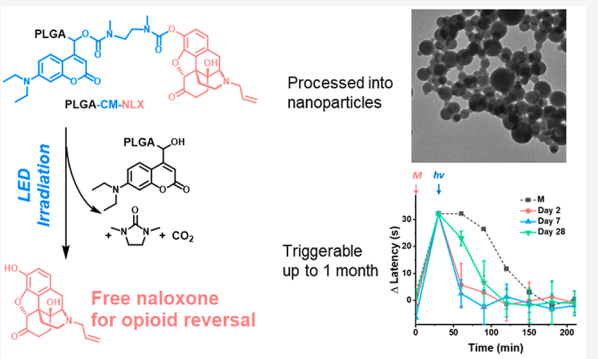


**KEYWORDS:** *Stimulus-responsive, photocleave, drug delivery, prodrug, naloxone, opioid*



There are more than 40 000 deaths from opioid overdose each year in the U.S.[1] Timely treatment with an opioid antagonist such as naloxone (NLX) can be life-saving in opioid overdose.[2] Even though the importance of naloxone is recognized, factors limit access:[3] naloxone not being stocked by pharmacies,[4,5] restrictions to access by lay people,[6] affordability[7] and payment method, the stigma surrounding opioid use disorder,[8] and other socioeconomic factors. Even when acquired, naloxone may not be on the person needing it at the time of overdose.

Naloxone could be delivered by a sustained release system placed in the patient during contact with the healthcare system. However, prolonged constant release of naloxone could interfere with normal usage of opioids, such as in acute perioperative use or in treatment of opioid use disorder. A system that was injected into the patient at the time of contact with the healthcare system and that released naloxone only when needed would be a major advance.

Stimuli-responsive materials have been used to provide temporal control of drug delivery, in contrast to the extended release from more conventional drug delivery systems.[9−12] Stimuli such as light,[13,14] temperature,[15,16] and ultrasound[17,18] have been employed in various applications. Light has been commonly used because of its ease of spatiotemporal control and tunability of wavelength and intensity.[19] As one example of an analogous application, we have used phototriggering to provide on-demand local anesthesia, where the timing, intensity, and duration of local anesthesia could be adjusted by modulating the intensity and/or duration of irradiation of an injected depot.[13,20]

Here, we designed a light-responsive polymer−naloxone conjugate and formulated it into injectable nanoparticles. Blue (400 nm) light was used since the drug depot would be injected subcutaneously (deep penetration by light would not be necessary) and because light of shorter wavelengths has a higher energy to cleave chemical bonds. Coumarin (CM) was used as the photocleavable linkage due to its good photocleavage efficiency with blue light.[13,19] The subcutaneously injected polymer−drug conjugate would not release naloxone unless the site was irradiated with light of a specific wavelength, at an irradiance far greater than that of ambient light.[21] Poly(lactic-*co*-glycolic acid) (PLGA) was selected as the polymeric carrier for naloxone. PLGA is an FDA-approved polymer that has been widely used in drug delivery.[22,23] Since the drugs were attached at the polymer chain ends, a low molecular weight (2000 Da) was selected to achieve a high drug loading (i.e., the ratio of total drug mass to polymer mass would be high).

**Received:** September 9, 2023
**Revised:** October 17, 2023
**Accepted:** October 17, 2023
**Published:** November 8, 2023

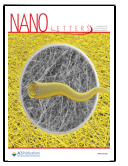

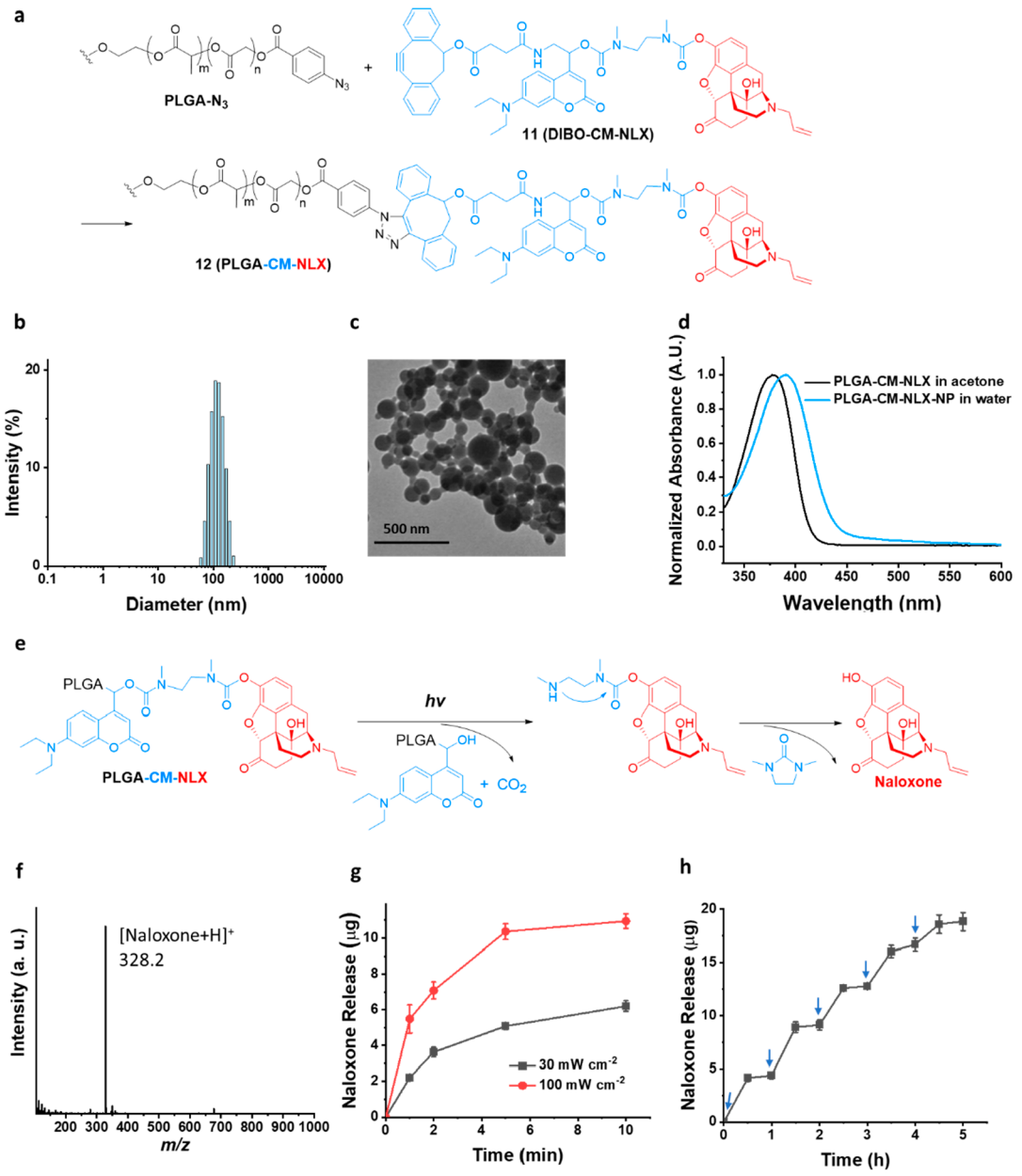


**Figure 1.** Synthesis, characterization, and in vitro photocleavage. (a) Synthesis of PLGA-CM-NLX. (b) DLS of the PLGA-CM-NLX nanoparticles. (c) TEM image of the PLGA-CM-NLX nanoparticles. (d) UV−vis spectra of the PLGA-CM-CM-NLX in acetone and nanoparticles in water. (e) Scheme of photocleavage releasing naloxone from PLGA-CM-NLX. (f) Mass spectrum of the cleaved naloxone. (g) Release of naloxone by photocleavage of NLX-NP (10 mg $mL^{-1}$) over time with a 400 nm LED at different irradiances ($n$ = 4, data are means ± SD). (h) Repeated phototriggered naloxone release from NLX-NP (arrows represent 2 min of irradiation with a 400 nm LED at 30 mW $cm^{-2}$, $n$ = 4, data are means ± SD).

**Synthesis and Characterization.** A polymer−naloxone conjugate (PLGA-CM-NLX) was synthesized (Figure 1a). The synthesis is detailed in Supplementary Figure 1. In brief, we synthesized a coumarin−naloxone conjugate with a dibenzocyclooctyne (DIBO) moiety, which was reacted with azide-terminated PLGA (molecular weight 2 kDa, lactide/glycolide 50:50) through strain-promoted azide−alkyne cycloaddition (SPAAC). Disappearance of the azide group at 2100 $cm^{-1}$ in Fourier-transform infrared (FT-IR) spectra confirmed the coupling (Supplementary Figure 2).[24,25] Representative peaks of polymer and drug were observed by nuclear magnetic resonance (NMR) spectroscopy (Supplementary Figure 3), e.g., 5.2 and 4.8 ppm from the lactic and glycolic moieties of PLGA, respectively, and 5.8 ppm from the vinyl moiety of naloxone. The retention time by gel permeation chromatography (GPC) of PLGA-CM-NLX was also shortened compared to PLGA-azide, indicating increased molecular size and weight (Supplementary Figure 4). We used SPAAC rather than copper-catalyzed azide−alkyne cycloaddition because it is highly efficient for macromolecules, and reaction conditions are mild and do not require catalysts without metal residue.[26−28]

PLGA-CM-NLX was dissolved in acetone, and 103 ± 29 nm (by dynamic light scattering (DLS; Figure 1b) nanoparticles


https://doi.org/10.1021/acs.nanolett.3c03426
Nano Lett. 2023, 23, 10545−10553

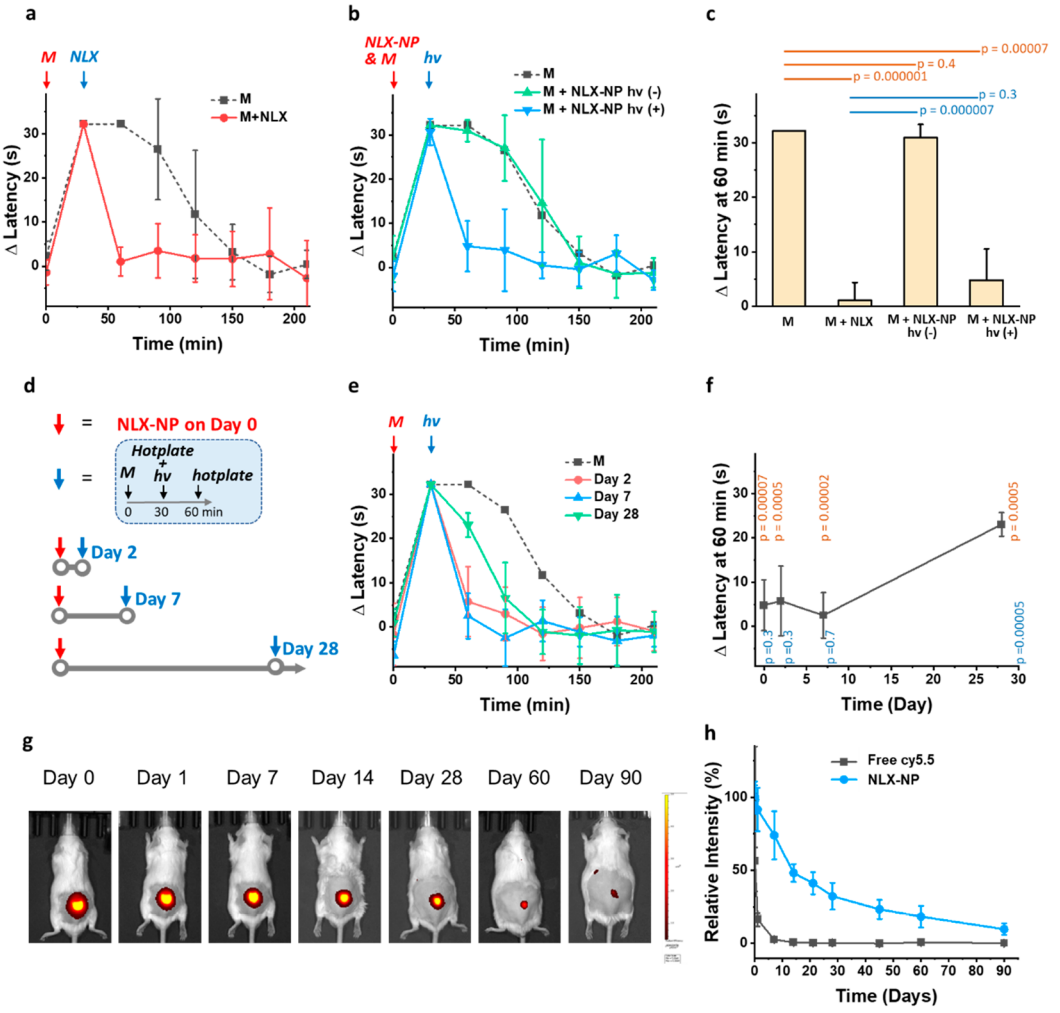


**Figure 2.** In vivo reversal of opioid effect by NLX-NP. Hot plate Δ latency of mice injected subcutaneously with morphine (a) Without (M, black line) or with (M+NLX, red line) naloxone injection at 30 min (b) With injected NLX-NP at $t$ = 0 min, without ((M+NLX-NP $h\nu$ (−)), green line), or with ((M+NLX-NP $h\nu$ (+)), blue line) subsequent irradiation at 30 min. (c) Δ latency at 60 min from data in panels a and b. (d) Illustration of experimental timeline for delayed triggering; see the text for details. (e) Hot plate Δ latency of mice treated with morphine at the indicated time after injection of NLX-NP, followed by irradiation. (f) Δ latency at 60 min after morphine and 30 min after irradiation (from data in panels b and e) as a function of days after injection of NLX-NP. $p$ values in yellow compare the Δ latencies of irradiated animals to animals 60 min after morphine; the $p$ values in blue compare the Δ latencies of irradiated animals to those 30 min after free naloxone. (g) In vivo imaging system (IVIS) images of mice injected with NLX-NP containing PLGA covalently labeled with the fluorescent dye cyanine 5.5 (PLGA-cy5.5). (h) Quantitation of relative fluorescent intensity over time from IVIS data in panel g; see Supplementary Figure 9 for images for the free dye. All irradiations ($h\nu$) in this figure were for 2 min with a 400 nm LED at 300 mW cm$^{-2}$. The black dashed lines in panels a, b, and e are the curves for morphine alone. All data are means ± SD, $n$ = 4.

(NLX-NP) were prepared by nanoprecipitation into water. Spherical nanoparticles were observed by transmission electron microscopy (TEM; Figure 1c). PLGA-CM-NLX in acetone showed a representative UV−vis absorption peak at 378 nm from the coumarin moiety. The peak shifted to 392 nm when nanoparticles formed (Figure 1d). This red-shift can be attributed to aggregation of molecules in the solid form.[29]

NLX-NP irradiated with 400 nm light cleaved to a naloxone derivative, which released unmodified naloxone by self-immolative cyclization[30,31] (Figure 1e). Release of unmodified naloxone ($m/z$ 328.2; Figure 1f) was confirmed by liquid chromatography−mass spectroscopy (LC-MS). Naloxone release from NLX-NP increased with duration or intensity of irradiation with a 400 nm LED (Figure 1g). Naloxone release from NLX-NP could be repeatedly triggered by irradiation (Figure 1h).

**In Vivo Efficacy.** The effectiveness of light-triggered naloxone was assessed in mice using a hot plate test, widely used for testing opioid analgesia.[32−34] Dosing was constant throughout: 10 mg kg$^{-1}$ for morphine, 0.1 mg kg$^{-1}$ for naloxone, 100 mg kg$^{-1}$ for NLX-NP, and 300 mW cm$^{-2}$ for 2 min for irradiation events with a 400 nm LED.

At predetermined intervals (every 30 min), animals were placed on a 50 °C hot plate, and the latency (time in seconds) to a response (flinching, licking their hind paws, or jumping) was recorded every 30 min except where indicated otherwise. Latency of animals without treatment with morphine (baseline) was 27.8 ± 4.7 s. This baseline was used to calculate Δ latency: the difference between the latency in treated animals and the baseline. Latency of animals treated with morphine (subcutaneously between the scapulae) rose to 60 s by 30 min after injection, with a Δ latency of 32.2 s (Figure 2a). (Since


https://doi.org/10.1021/acs.nanolett.3c03426
Nano Lett. 2023, 23, 10545−10553

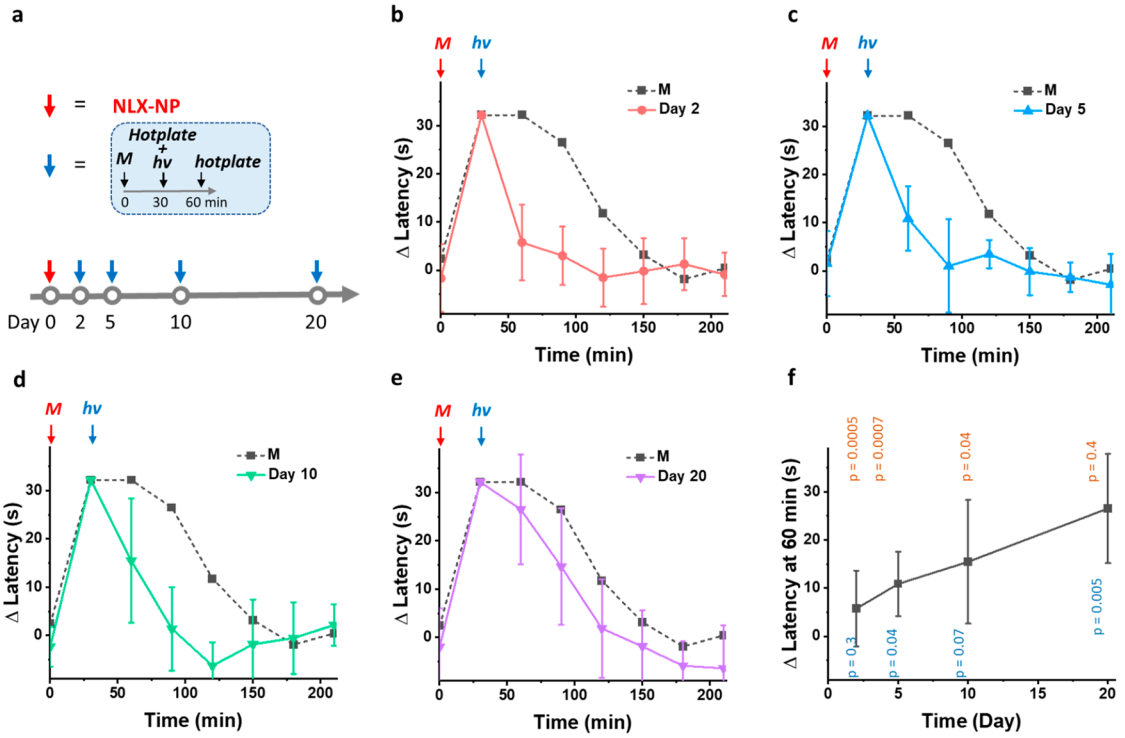


**Figure 3.** Repeated triggering. (a) Illustration of the experimental timeline. Hot plate Δ latency of mice injected with NLX-NP then, at predetermined intervals, administered morphine, followed 30 min later by irradiation. (b) Latencies on day 2; (c) day 5; (d) day 10; (e) day 20 ($h\nu$: 2 min of irradiation by 400 nm LED at 300 mW cm$^{-2}$; the black dashed line is the curve for morphine; data are means ± SD, $n$ = 4). (f) Δ latency at 60 min after morphine injection (from panels b–e) as a function of time after injection. $p$ values in yellow are compared to Δ latency in the morphine only group; $p$ values in blue are compared to morphine treated with free naloxone.

animals were removed from the hot plate at 60 s to avoid thermal injury, 60 s was the maximum latency. Therefore, the maximum Δ latency from the test was 32.2 s.) The Δ latency remained 32.2 s at 60 min and gradually returned to the baseline at difference of 174.5 ± 50.0 min.

When animals treated with morphine (Δ latency = 32.2 s) were administered free naloxone subcutaneously 30 min after the morphine (but at a different site in the lower back), the Δ latency decreased to 1.1 ± 3.3 s at the next time point (60 min; $p$ = 0.000001, Figure 2a) and remained at the baseline afterward, indicating that free naloxone reversed the effect of morphine for the entirety of the opioid's duration of effect.

We tested the ability of NLX-NP to provide triggered opioid reversal. NLX-NP (100 mg kg$^{-1}$, containing 300 μg NLX) was injected subcutaneously in the lower back of mice, followed immediately by the injection of morphine subcutaneously between the scapulae. In the absence of irradiation of the site of NLX-NP injection, Δ latency remained at 30.7 ± 3.0 s (Figure 2b) 30 min after morphine injection, similar to the latencies in mice injected with morphine only, indicating that naloxone linked to the polymer was not released. When the site of NLX-NP injection was irradiated with a 400 nm LED for 2 min at 300 mW cm$^{-2}$ 30 min after morphine, Δ latency decreased to 4.8 ± 5.7 s at 60 min (Figure 2b; $p$ = 0.00007), similar to that in morphine-treated animals treated with free naloxone at the same time point ($p$ = 0.3). These data indicated that irradiation released naloxone and reversed the effect of the opioid. We measured that approximately 6.7 ± 0.7% of light from the LED could penetrate skin to the subcutaneous site of injection.

To determine effect onset time, animals were injected with morphine, then 30 min later injected with free naloxone or NLX-NP and then triggered with 400 nm light and tested every 5 min (Supplementary Figure 7). The onset time of reversal by naloxone triggered from NLX-NP was slightly slower than that from free naloxone. With free naloxone, it took 5 min for Δ latency to become different from that of animals treated with morphine alone ($p$ = 0.03); with triggered release of naloxone, this took 10 min ($p$ = 0.04). With free naloxone, latency was similar to the baseline within 10 min ($p$ = 0.08); with a triggered release of naloxone, this took 20 min ($p$ = 0.06).

In clinical applications, the depot would be injected subcutaneously by healthcare practitioners and only triggered in emergencies at a later time. We assessed the potential for late triggering by injecting NLX-NP on day 0 without irradiation. At predetermined intervals after injection of NLX-NP (2 days, 1 week, or 1 month, Figure 2d), separate groups of animals were first injected with morphine, then 30 min later, after the Δ latency had risen to the maximum (32.2 s), they were irradiated with a 400 nm LED at 300 mW cm$^{-2}$ for 2 min at the site of NLX-NP injection. Latency was measured again 30 min later, to assess the effect of the phototriggered release of naloxone (Figure 2e,f). Two days after the injection of NLX-NP, irradiation reduced Δ latency from morphine from 32.2 s to 5.8 ± 7.9 s ($p$ = 0.0006), similar to the Δ latency with morphine treated with free naloxone ($p$ = 0.3, from Figure 2a; Figure 2e and f). Irradiation at 1 week reduced Δ latency from 32.2 s to 2.5 ± 5.1 s ($p$ = 0.00002; $p$ = 0.6 compared to the free naloxone group, from Figure 2a), and at 1 month, it reduced Δ latency from 32.2 to 23.1 ± 2.7 s, a


https://doi.org/10.1021/acs.nanolett.3c03426
Nano Lett. 2023, 23, 10545−10553

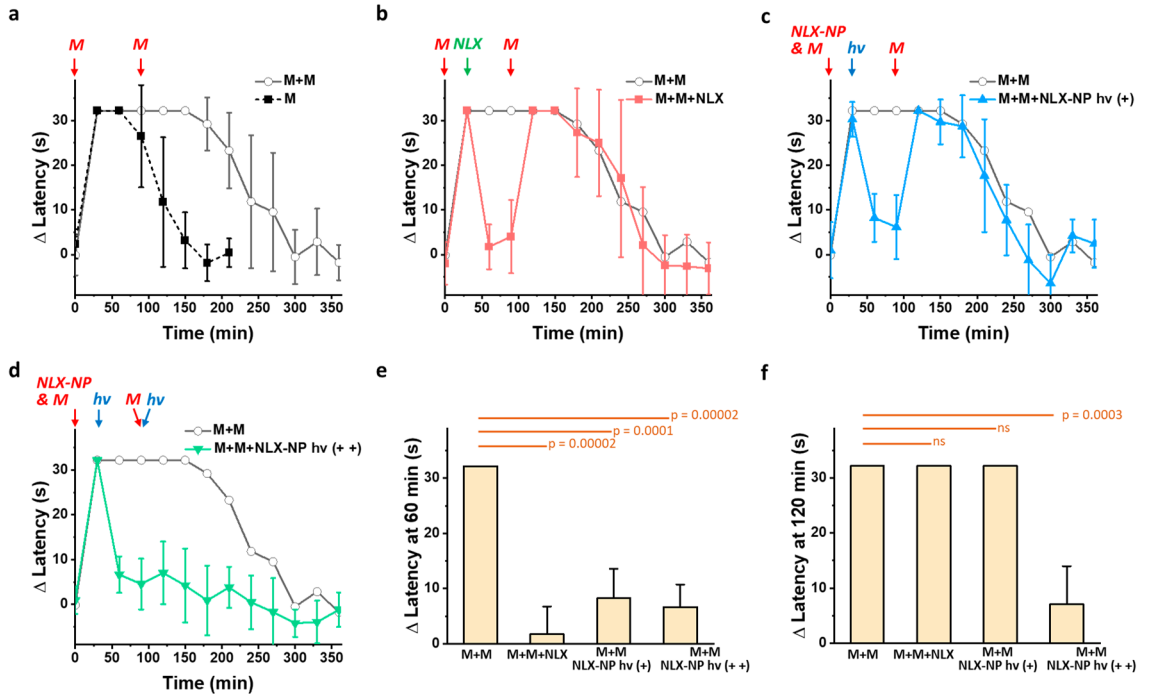


**Figure 4.** Triggered reversal of repeated doses of morphine. (a) Latency of mice receiving two sequential doses of morphine without other injections (M+M, the gray lines in all panels) vs mice receiving a single dose of morphine (M, dashed line). (b) Same experiment as panel a but with a single injection of naloxone at 30 min (M+M+NLX). (c) Same experiment as panel a but with NLX-NP injected at time 0 and one irradiation at 30 min (M+M+NLX-NP hv (+), *hν* = 2 min irradiation by 400 nm LED at 300 mW $cm^{-2}$). (d) Same experiment as panel c but with irradiations at 30 and 90 min (M+M+NLX-NP *hv* (++)). (e, f) Δ latencies at 60 min (e) and 120 min (f) from data in panels a−d. $n$ = 4, data are means ± SD.

lesser but statistically significant reduction ($p$ = 0.0005; $p$ = 0.00005 compared to the free naloxone group). NLX-NP did not show triggered opioid reversal if irradiation was performed two months after injection (Supplementary Figure 8). The ability to trigger long after injection was consistent with the demonstration with an in vivo imaging system (IVIS) that subcutaneously injected NLX-NP containing PLGA covalently labeled with the fluorescent dye cyanine5.5 (PLGA-cy5.5) remained in tissue for at least a month (Figure 2g and h). This prolonged retention can be attributed to the nanoparticles, since most of the fluorescent signal of injected free y5.5 disappeared within 1 day (Supplementary Figure 9).

Repeated dosing with naloxone could be important for eventual clinical application, to extend the useful lifetime of the device. Repeated dosing was studied by injecting animals with NLX-NP and testing the ability to trigger the reversal of morphine on days 2, 5, 10, and 20 in the same animals (Figure 3). The Δ latencies after triggering at 2, 5, and 10 days were 5.8 ± 7.9, 10.9 ± 6.7, and 15.5 ± 12.9 s, respectively, which were all statistically significantly reduced compared to Δ latencies before irradiation (32.2 s, $p$ = 0.0005, 0.0007, and 0.04, respectively). Triggering on day 20 (26.5 ± 11.4 s) did not reduce Δ latency ($p$ = 0.36 compared to Δ latency before irradiation).

Repeated dosing with naloxone would be important in the case of opioid overdose with a dose that had a prolonged effect. We mimicked that situation by the repeated administration of morphine. After the initial dose of morphine, a second dose was given at 90 min, while the latency remained near-maximal. The combined morphine doses produced analgesia for 5 h (the time until latency was no longer statistically significantly different from baseline), compared to 2 h from a single dose of morphine (Figure 4a). A dose of free naloxone injected 30 min after the first dose of morphine decreased Δ latency from 32.2 s to 1.7 ± 5.0 s (Figure 4b and e, $p$ = 0.00002). With a second dose of morphine at 90 min, Δ latency rose to 32.2 s; i.e., the effect of morphine was not impeded by the previously administered naloxone (Figure 4b). Similarly, in animals injected with NLX-NP at the same time as the initial dose of morphine ($t$ = 0 min), irradiation of the nanoparticles at 30 min reversed the effect of morphine but did not prevent the effect of the second dose of morphine (Figure 4c). A second irradiation at 90 min prevented the effect of the second dose of morphine (Figure 4d and f) with the Δ latency remaining at 7.0 ± 7.0 s ($p$ = 0.0003 compared to 32.2s for animals that did not receive the second irradiation) at the next time point (i.e., 120 min), demonstrating that a prolonged morphine effect could be reversed by repeated triggering.

**Cytotoxicity and Biocompatibility.** NLX-NP showed minimal or no cytotoxicity in 3T3 fibroblasts or C2C12 muscle cells (Supplementary Figure 10, $p$ > 0.05 compared to the saline group). Naloxone also showed minimal cytotoxicity below 0.5 mg $mL^{-1}$ in both cell lines ($p$ > 0.05 compared to the saline group), but cell survival was reduced to 76.0 ± 10.5% at 1 mg $mL^{-1}$ for 3T3 cells (p = 0.007 compared to the saline group) and 80.0 ± 5.2% cell survival for C2C12 cells ($p$ = 0.0005 compared to the saline group).

To assess tissue reaction *in vivo*, animals were euthanized 4, 14, or 30 days following subcutaneous injection of NLX-NP. The tissues around the site of injection, including epidermis, dermis, dermal white adipose tissue (dWAT), panniculus carnosus (a subcutaneous muscle layer found in mice but not


https://doi.org/10.1021/acs.nanolett.3c03426
Nano Lett. 2023, 23, 10545−10553

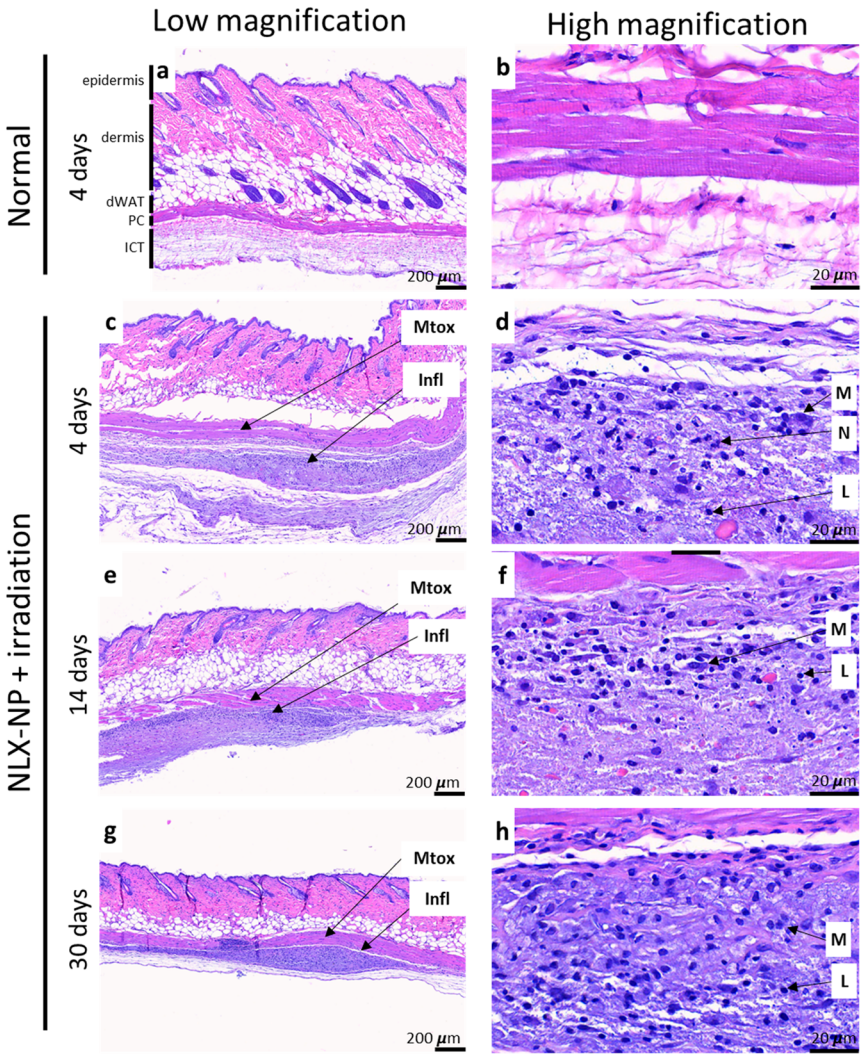


**Figure 5.** Tissue reaction to subcutaneously injected PLGA-CM-NLX NP. (a, b) Normal tissues. (c–h) Tissue reaction to the materials 4, 14, and 30 days after the injection. dWAT, dermal white adipose tissue; PC, panniculus carnosus; ICT, interstitial connective tissue; Mtox, myotoxicity; Infl, inflammation; M, macrophages; N, neutrophils; L, lymphocytes.

humans), and interstitial connective tissue, were processed into hematoxylin and eosin (H&E) stained slides (Figure 5).

Four days after injection and irradiation, mild to moderate inflammation with occasional neutrophils and more lymphocytes and macrophages occurred in tissues adjacent to the area of particle deposition, specifically the panniculus carnosus and interstitial connective tissue (Figure 5c,d). The depth of injection was 664 ± 79 μm. More superficial tissues, including the epidermis, dermis, and dWAT, did not demonstrate inflammation or cell injury. Inflammation was diminished by days 14 and 30 (Figure 5e-h), consisting principally of lymphocytes and foamy macrophages (reflecting the uptake of injected particles). Tissues from animals injected with NLX-NP without irradiation showed similar inflammation (Supplementary Figure S11), indicating that irradiation was not the source of inflammation.

On day 4, there was very mild myotoxicity of the panniculus carnosus, with regenerating myocytes adjacent to the area of particle deposition (i.e., interstitial connective tissue) as well as myocytes with nuclear internalization (Figure 5d). The superficial layers of the panniculus carnosus (i.e., those further away from NLX-NP) had no myotoxicity. The panniculus is not found in humans. By days 14 (Figure 5f) and 30 (Figure 5h), myotoxicity was overall diminished with myocytes demonstrating regeneration, and no necrosis was observed. Histology from animals injected with NLX-NP but not irradiated were similar to those that were (Supplementary Figure S11).

We developed a polymer–naloxone depot to provide light-triggered reversal of opioid effects. For many externally triggered drug delivery systems (e.g., those based on hydrogels or particles, such as liposomes), substantial untriggered drug release is not uncommon; it may result in untriggered therapeutic effects. Here, the NLX-NP was inert and did not interfere with the effect of morphine. The system only released naloxone when irradiated, and could reverse the opioid effect. Minimal untriggered drug release from a depot is desirable in the design of an externally triggered naloxone-releasing system to minimize the loss of drug that could be used in triggered events and to avoid interfering with the therapeutic usage of opioids.

We used morphine analgesia in mice as a model and a proxy for opioid overdose. Opioid overdose occurs by the same pharmacological mechanism (i.e., the same opioid receptors)


https://doi.org/10.1021/acs.nanolett.3c03426
Nano Lett. 2023, 23, 10545–10553

as opioid-induced analgesia. Moreover, since the dose used here to induce analgesia in mice (10 mg $kg^{-1}$) is approximately 100-fold greater than a substantial analgesic dose in humans (0.1 mg $kg^{-1}$), the ability to reverse murine opioid analgesia reflects the ability to reverse a very large opioid dose.

The therapeutic index of naloxone is high.[2] There would therefore be few adverse effects of overtriggering other than possibly inducing opioid withdrawal in addicted users, a necessary risk of treating overdoses. Accidental triggering by ambient light is unlikely since the irradiance required for triggering is ∼100-fold greater.[21,35] If necessary, in clinical practice, the device might be protected from ambient light. The LED could be readily incorporated into a personal adornment, such as jewelry, or in a MedicAlert bracelet, possibly overlying the site of injection.

The device would be administered by health care professionals and would subsequently be on the patient's person, obviating issues with access to naloxone,[4,5] and removing the need to find or carry intranasal naloxone delivery systems.

The materials remained triggerable for up to a month after initial administration due to the long retention of the PLGA. In clinical practice, the system would be administered by the healthcare system. The naloxone depot would be activated only when needed at a remote and unpredictable time. Overdose might require more than one dose of naloxone for successful rescue. Since the half-life of the opioid used may be longer than that of naloxone,[36] repeated triggering may be necessary. Overdose could also occur on more than one occasion. We have demonstrated that our system could provide a rescue in those circumstances. In this proof-of-principle study, opioid reversal could not be triggered two months after injection. An eventual clinical system could be engineered to provide more doses of naloxone over a longer period.

U.S. FDA-approved intranasal, intramuscular, and subcutaneous systems for naloxone delivery exist.[37] All three methods can achieve effective bioavailability within 15−20 min. The onset of the triggered reversal of morphine with NLX-NP occurred within that time frame. Further optimization in dosage, formulation, or irradiation could accelerate naloxone release.

Tissue reaction to NLX-NP was consistent with reaction to injected polymeric materials,[38,39] except that PLGA itself generally does not cause myotoxicity; the myotoxicity might due to the low molecular weight polymer or the small size of the particles,[40,41] or a combination of PLGA with even low doses of therapeutics.[42] NLX-NP would be used subcutaneously in humans, where there is no equivalent to the murine panniculus carnosus (where myotoxicity was seen). Therefore, the myotoxicity is likely a nonissue from the clinical point of view.

In summary, we have developed a light-responsive polymer−naloxone conjugate that was processed into injectable nanoparticles and could release naloxone in its native form upon blue light irradiation. The material did not affect opioid effect in the absence of phototriggering but enabled opioid reversal by light irradiation. Triggering could be performed weeks after administration, over multiple days and multiple times. The material could provide on-demand opioid antidote administration to reverse overdoses.

## ■ ASSOCIATED CONTENT

### Supporting Information

The Supporting Information is available free of charge at https://pubs.acs.org/doi/10.1021/acs.nanolett.3c03426.

Experimental details, materials, and methods, and additional data, including $^1$H NMR of all compounds, GPC, FTIR, additional histology, and in vitro and in vivo characterizations (PDF)

## ■ AUTHOR INFORMATION


### Corresponding Author

**Daniel S. Kohane** − *Laboratory for Biomaterials and Drug Delivery, The Department of Anesthesiology, Critical Care and Pain Medicine, Boston Children's Hospital, Harvard Medical School, Boston, Massachusetts 02115, United States*; Email: daniel.kohane@childrens.harvard.edu

### Authors

**Wei Zhang** − *Laboratory for Biomaterials and Drug Delivery, The Department of Anesthesiology, Critical Care and Pain Medicine, Boston Children's Hospital, Harvard Medical School, Boston, Massachusetts 02115, United States*

**Dali Wang** − *Laboratory for Biomaterials and Drug Delivery, The Department of Anesthesiology, Critical Care and Pain Medicine, Boston Children's Hospital, Harvard Medical School, Boston, Massachusetts 02115, United States*

**Claire A. Ostertag-Hill** − *Laboratory for Biomaterials and Drug Delivery, The Department of Anesthesiology, Critical Care and Pain Medicine, Boston Children's Hospital, Harvard Medical School, Boston, Massachusetts 02115, United States*

**Yiyuan Han** − *Laboratory for Biomaterials and Drug Delivery, The Department of Anesthesiology, Critical Care and Pain Medicine, Boston Children's Hospital, Harvard Medical School, Boston, Massachusetts 02115, United States*

**Xiyu Li** − *Laboratory for Biomaterials and Drug Delivery, The Department of Anesthesiology, Critical Care and Pain Medicine, Boston Children's Hospital, Harvard Medical School, Boston, Massachusetts 02115, United States*

**Yueqin Zheng** − *Laboratory for Biomaterials and Drug Delivery, The Department of Anesthesiology, Critical Care and Pain Medicine, Boston Children's Hospital, Harvard Medical School, Boston, Massachusetts 02115, United States*

**Berwyn Lu** − *Laboratory for Biomaterials and Drug Delivery, The Department of Anesthesiology, Critical Care and Pain Medicine, Boston Children's Hospital, Harvard Medical School, Boston, Massachusetts 02115, United States*

Complete contact information is available at: https://pubs.acs.org/10.1021/acs.nanolett.3c03426


### Notes

The authors declare no competing financial interest.

## ■ ACKNOWLEDGMENTS

This study was supported by the National Institutes of Health (NIH) grants R35GM131728 and K99GM141269 and by the CHMC Anesthesia Foundation Inc.

## ■ REFERENCES

(1) Florence, C.; Luo, F.; Rice, K. The economic burden of opioid use disorder and fatal opioid overdose in the United States, 2017. *Drug and Alcohol Dependence* **2021**, *218*, No. 108350.

(2) Wermeling, D. P. Review of naloxone safety for opioid overdose: practical considerations for new technology and expanded public access. *Ther. Adv. Drug Saf.* **2015**, *6* (1), 20−31.
(3) Ong, A. R.; Lee, S.; Bonar, E. E. Understanding disparities in access to naloxone among people who inject drugs in Southeast Michigan using respondent driven sampling. *Drug and Alcohol Dependence* **2020**, *206*, No. 107743.
(4) Houser, R. Expanding Access to Naloxone: A Necessary Step to Curb the Opioid Epidemic. *Disaster Medicine and Public Health Preparedness* **2023**, *17*, No. e245.
(5) Pollini, R. A.; Ozga, J. E.; Joyce, R.; Xuan, Z.; Walley, A. Y. Limited access to pharmacy-based naloxone in West Virginia: Results from a statewide purchase trial. *Drug and Alcohol Dependence* **2022**, *231*, No. 109259.
(6) Meyerson, B. E.; Moehling, T. J.; Agley, J. D.; Coles, H. B.; Phillips, J. Insufficient access: naloxone availability to laypeople in Arizona and Indiana, 2018. *J. of Health Care for the Poor and Underserved* **2021**, *32* (2), 819−829.
(7) Connolly, E.; McCall, K. L.; Couture, S.; Felton, M.; Piper, B. J.; Bratberg, J. P.; Tu, C. Analysis of naloxone access and primary medication nonadherence in a community pharmacy setting. *J. Am. Pharm. Assoc.* **2022**, *62* (1), 49−54.
(8) Adeosun, S. O. Stigma by association: to what extent is the attitude toward naloxone affected by the stigma of opioid use disorder? *J. Pharm. Pract.* **2023**, *36* (4), 941−952.
(9) Zhang, W.; Kohane, D. S. Keeping Nanomedicine on Target. *Nano Lett.* **2021**, *21* (1), 3−5.
(10) Wang, Y.; Kohane, D. S. External triggering and triggered targeting strategies for drug delivery. *Nat. Rev. Mater.* **2017**, *2*, 17020.
(11) Mura, S.; Nicolas, J.; Couvreur, P. Stimuli-responsive nanocarriers for drug delivery. *Nat. Mater.* **2013**, *12* (11), 991−1003.
(12) Fleige, E.; Quadir, M. A.; Haag, R. Stimuli-responsive polymeric nanocarriers for the controlled transport of active compounds: Concepts and applications. *Adv. Drug Delivery Rev.* **2012**, *64* (9), 866−884.
(13) Zhang, W.; Ji, T.; Li, Y.; Zheng, Y.; Mehta, M.; Zhao, C.; Liu, A.; Kohane, D. S. Light-triggered release of conventional local anesthetics from a macromolecular prodrug for on-demand local anesthesia. *Nat. Commun.* **2020**, *11* (1), 2323.
(14) Wang, Z.; Ju, Y.; Ali, Z.; Yin, H.; Sheng, F.; Lin, J.; Wang, B.; Hou, Y. Near-infrared light and tumor microenvironment dual responsive size-switchable nanocapsules for multimodal tumor theranostics. *Nat. Commun.* **2019**, *10* (1), 4418.
(15) Hogan, K. J.; Mikos, A. G. Biodegradable thermoresponsive polymers: Applications in drug delivery and tissue engineering. *Polymer* **2020**, *211*, No. 123063.
(16) Gupta, M. K.; Martin, J. R.; Werfel, T. A.; Shen, T.; Page, J. M.; Duvall, C. L. Cell Protective, ABC Triblock Polymer-Based Thermoresponsive Hydrogels with ROS-Triggered Degradation and Drug Release. *J. Am. Chem. Soc.* **2014**, *136* (42), 14896−14902.
(17) Sirsi, S. R.; Borden, M. A. State-of-the-art materials for ultrasound-triggered drug delivery. *Adv. Drug Delivery Rev.* **2014**, *72*, 3−14.
(18) Yan, F.; Li, L.; Deng, Z.; Jin, Q.; Chen, J.; Yang, W.; Yeh, C.-K.; Wu, J.; Shandas, R.; Liu, X.; Zheng, H. Paclitaxel-liposome−microbubble complexes as ultrasound-triggered therapeutic drug delivery carriers. *J. Controlled Release* **2013**, *166* (3), 246−255.
(19) Xiao, P.; Zhang, J.; Zhao, J.; Stenzel, M. H. Light-induced release of molecules from polymers. *Prog. Polym. Sci.* **2017**, *74*, 1−33.
(20) Rwei, A. Y.; Lee, J.-J.; Zhan, C.; Liu, Q.; Ok, M. T.; Shankarappa, S. A.; Langer, R.; Kohane, D. S. Repeatable and adjustable on-demand sciatic nerve block with phototriggerable liposomes. *Proc. Natl. Acad. Sci. U. S. A.* **2015**, *112* (51), 15719−15724.
(21) Jeanmougin, M.; Civatte, J. Dosimetry of solar ultraviolet radiation. Daily and monthly changes in Paris. *Ann. Dermatol. Venereol.* **1987**, *114* (5), 671−676.
(22) Danhier, F.; Ansorena, E.; Silva, J. M.; Coco, R.; Le Breton, A.; Préat, V. PLGA-based nanoparticles: An overview of biomedical applications. *J. Controlled Release* **2012**, *161* (2), 505−522.
(23) Park, K.; Skidmore, S.; Hadar, J.; Garner, J.; Park, H.; Otte, A.; Soh, B. K.; Yoon, G.; Yu, D.; Yun, Y.; Lee, B. K.; Jiang, X.; Wang, Y. Injectable, long-acting PLGA formulations: Analyzing PLGA and understanding microparticle formation. *J. Controlled Release* **2019**, *304*, 125−134.
(24) Zhang, W.; Huang, M.; Su, H.; Zhang, S.; Yue, K.; Dong, X.-H.; Li, X.; Liu, H.; Zhang, S.; Wesdemiotis, C.; Lotz, B.; Zhang, W.-B.; Li, Y.; Cheng, S. Z. D. Toward Controlled Hierarchical Heterogeneities in Giant Molecules with Precisely Arranged Nano Building Blocks. *ACS Cent. Sci.* **2016**, *2* (1), 48−54.
(25) Zhang, W.; Chu, Y.; Mu, G.; Eghtesadi, S. A.; Liu, Y.; Zhou, Z.; Lu, X.; Kashfipour, M. A.; Lillard, R. S.; Yue, K.; Liu, T.; Cheng, S. Z. D. Rationally Controlling the Self-Assembly Behavior of Triarmed POSS−Organic Hybrid Macromolecules: From Giant Surfactants to Macroions. *Macromolecules* **2017**, *50* (13), 5042−5050.
(26) Tang, W.; Becker, M. L. "Click" reactions: a versatile toolbox for the synthesis of peptide-conjugates. *Chem. Soc. Rev.* **2014**, *43* (20), 7013−7039.
(27) Sletten, E. M.; Bertozzi, C. R. From Mechanism to Mouse: A Tale of Two Bioorthogonal Reactions. *Acc. Chem. Res.* **2011**, *44* (9), 666−676.
(28) Li, Y.; Dong, X.-H.; Zou, Y.; Wang, Z.; Yue, K.; Huang, M.; Liu, H.; Feng, X.; Lin, Z.; Zhang, W.; Zhang, W.-B.; Cheng, S. Z. D. Polyhedral oligomeric silsesquioxane meets "click" chemistry: Rational design and facile preparation of functional hybrid materials. *Polymer* **2017**, *125*, 303−329.
(29) Jin, H.; Zhang, W.; Wang, D.; Chu, Z.; Shen, Z.; Zou, D.; Fan, X.; Zhou, Q. Dendron-Jacketed Electrophosphorescent Copolymers: Improved Efficiency and Tunable Emission Color by Partial Energy Transfer. *Macromolecules* **2011**, *44* (24), 9556−9564.
(30) He, X.; Zhang, J.; Li, C.; Zhang, Y.; Lu, Y.; Zhang, Y.; Liu, L.; Ruan, C.; Chen, Q.; Chen, X.; Guo, Q.; Sun, T.; Cheng, J.; Jiang, C. Enhanced bioreduction-responsive diselenide-based dimeric prodrug nanoparticles for triple negative breast cancer therapy. *Theranostics* **2018**, *8* (18), 4884−4897.
(31) Weinstain, R.; Segal, E.; Satchi-Fainaro, R.; Shabat, D. Real-time monitoring of drug release. *Chem. Commun.* **2010**, *46* (4), 553−555.
(32) Lewanowitsch, T.; Irvine, R. J. Naloxone methiodide reverses opioid-induced respiratory depression and analgesia without withdrawal. *Eur. J. Pharmacol.* **2002**, *445* (1), 61−67.
(33) Suzuki, T.; Tsuji, M.; Mori, T.; Misawa, M.; Nagase, H. Involvement of $\delta$1 and $\delta$2 Opioid Receptor Subtypes in the Development of Physical Dependence on Morphine in Mice. *Pharmacol., Biochem. Behav.* **1997**, *57* (1), 293−299.
(34) Sora, I.; Takahashi, N.; Funada, M.; Ujike, H.; Revay, R. S.; Donovan, D. M.; Miner, L. L.; Uhl, G. R. Opiate receptor knockout mice define $\mu$ receptor roles in endogenous nociceptive responses and morphine-induced analgesia. *Proc. Natl. Acad. Sci. U. S. A.* **1997**, *94* (4), 1544−1549.
(35) Balasaraswathy, P.; Kumar, U.; Srinivas, C.; Nair, S. UVA and UVB in sunlight, optimal utilization of UV rays in sunlight for phototherapy. *Indian J. Dermatol. Venereol. Leprol.* **2002**, *68*, 198.
(36) Rzasa Lynn, R.; Galinkin, J. L. Naloxone dosage for opioid reversal: current evidence and clinical implications. *Ther. Adv. Drug Saf.* **2018**, *9* (1), 63−88.
(37) Ryan, S. A.; Dunne, R. B. J. P. m. Pharmacokinetic properties of intranasal and injectable formulations of naloxone for community use: a systematic review. *Pain Management* **2018**, *8* (3), 231−245.
(38) Anderson, J. M. In vivo biocompatibility of implantable delivery systems and biomaterials. *Eur. J. Pharm. Biopharm.* **1994**, *40* (1), 1−8.
(39) Kohane, D. S.; Lipp, M.; Kinney, R. C.; Anthony, D. C.; Louis, D. N.; Lotan, N.; Langer, R. Biocompatibility of lipid-protein-sugar particles containing bupivacaine in the epineurium. *J. Biomed. Mater. Res.* **2002**, *59* (3), 450−459.


https://doi.org/10.1021/acs.nanolett.3c03426
*Nano Lett.* 2023, 23, 10545−10553

(40) Brazeau, G. A.; Sciame, M.; Al-Suwayeh, S. A.; Fattal, E. J. P. D. Technology, Evaluation of PLGA microsphere size effect on myotoxicity using the isolated rodent skeletal muscle model. *Pharm. Dev. Technol.* **1996**, *1* (3), 279−283.
(41) Xiong, S.; George, S.; Yu, H.; Damoiseaux, R.; France, B.; Ng, K. W.; Loo, J. S.-C. Size influences the cytotoxicity of poly (lactic-co-glycolic acid)(PLGA) and titanium dioxide (TiO 2) nanoparticles. *Arch. Toxicol.* **2013**, *87*, 1075−1086.
(42) Padera, R.; Bellas, E.; Tse, J. Y.; Hao, D.; Kohane, D. S. Local myotoxicity from sustained release of bupivacaine from microparticles. *Anesthesiology* **2008**, *108* (5), 921−928.



https://doi.org/10.1021/acs.nanolett.3c03426
*Nano Lett.* 2023, 23, 10545−10553